Appendix to the NPDGamma Proposal

December 1999

1 Systematic effects for the NPDGamma experiment

The systematic effects relevant to the NPDGamma experiment are described in Section 4 of the NPDGamma proposal. The purpose of this appendix is to elucidate these effects and to describe a series of auxiliary measurements which will be performed to verify the size of the effects which are relevant to the NPDGamma experiment.

In order to understand a number of the systematic effects, it will be necessary to understand the time structure of the NPDGamma data. Consequently, the first section of this appendix will be a discussion of the time structure of the NPDGamma data, which is a reflection of the 20Hz proton beam repetition rate on the neutron spallation source and the 15m neutron flight path from the spallation source to the liquid para-hydrogen target. The neutron flux on the NPDGamma target as a function of neutron time of flight is shown in figure 1. This flux is for the conditions listed in section 3 of the proposal; namely, a 200microAmp proton beam, a 12.5cm by 12.5cm partially coupled liquid hydrogen moderator, a 3 theta critical neutron guide with dimensions of 12m in length and an area of 9.5cm by 9.5cm, and a 5atm-cm ^{3}He cell polarized to 65%. Also shown in figure 1 is the polarization of the neutron beam due to its passage through the polarized ^{3}He spin filter cell.

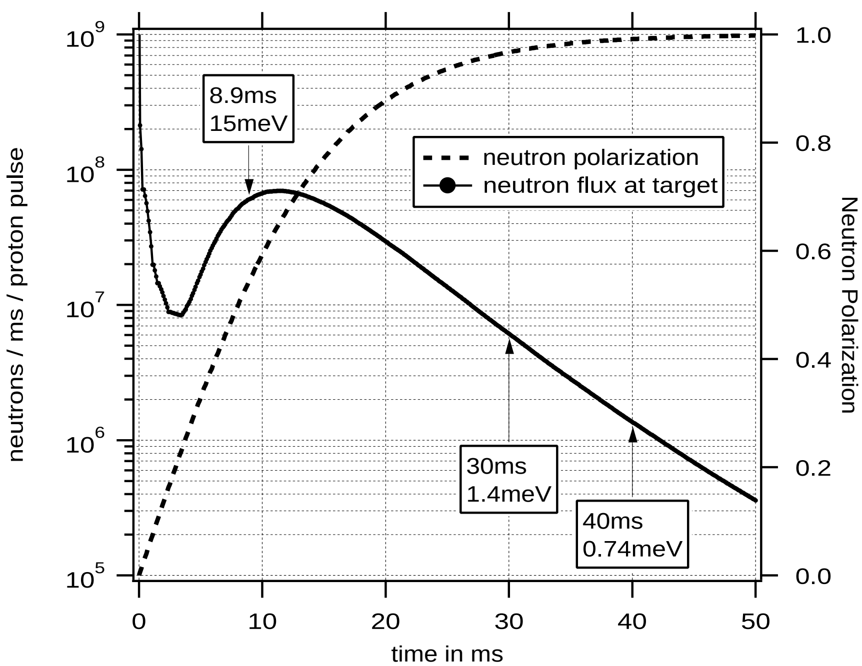

Figure 1: Neutron Flux for the NPDGamma Experiment

Using the capture efficiency of the hydrogen target (approximately 65%), the number of gammas produced in the hydrogen target as a function of neutron time of flight is shown in figure 2. These gammas from the parity violating NPDGamma reaction dominate the observed gammas in the CsI detectors. For comparison, the number of gammas which would be produced in a 2mm aluminum cryostat window are also shown in

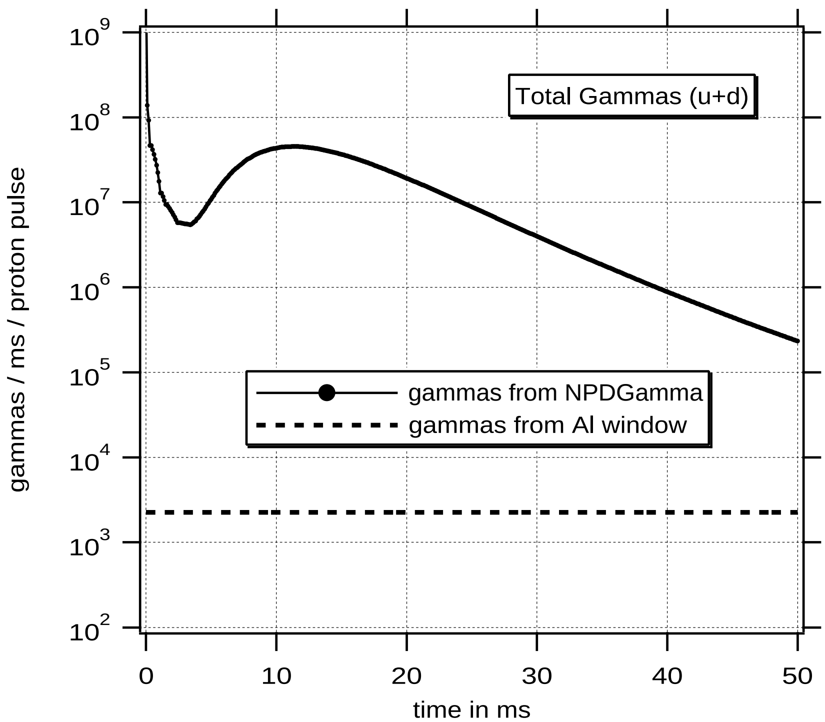

Figure 2: Gamma Production in the Hydrogen Target

figure 2. These gammas are the result of the cryostat window becoming activated by the neutron beam and then undergoing a beta decay. However, while the number of gammas from the cryostat window is many orders of magnitude smaller than the number of gammas from the NPDGamma reaction, the asymmetry of beta decay is many orders of magnitude larger than the asymmetry of the NPDGamma reaction and the gammas from the activated cryostat window can cause a measureable systematic effect. A more complete discussion of the cryostat window can be found in the next section. The large NPDGamma signal allows a measurement of the gamma asymmetry on the order of 10^{-4} with each proton pulse. With a running time of one year live, the NPDGamma experiment is capable of achieving a statistical error on the order of 5×10^{-9}. One factor which will determine the final error of the NPDGamma experiment is the time of flight window over which the data is integrated. NPDGamma data taking cannot begin before approximately 9ms as time of flights shorter than 9ms correspond to energies greater than 15meV. Above 15meV, the neutron is depolarized in the liquid para hydrogen target. Asymmetry data will be collected beginning at approximately 9ms, and continue until some cutoff time. The cutoff time will most likely be 30ms and will be implemented using a neutron time of flight chopper. Data collected for times less than 9ms will be for unpolarized neutrons and can be used as an *in situ* measurement of systematics. Likewise, data collected after the chopper cutoff time will be for zero neutron flux and can also be used for *in situ* systematic studies. Figure 3 shows the expected gamma asymmetry for the NPDGamma reaction, the statistical error per ms data collection bin for a year of running, and the integrated statistical error for a data collection window beginning at 9ms. The statistical error on the gamma asymmetry has reached a value of 4.7×10^{-9} by 30ms, and drops to only 4.5×10^{-9} by 50ms. Chopping the neutron beam at 30ms will have little effect on the statistical error of the gamma asymmetry and will allow a large time of flight window after 30ms for *in situ* systematic studies.

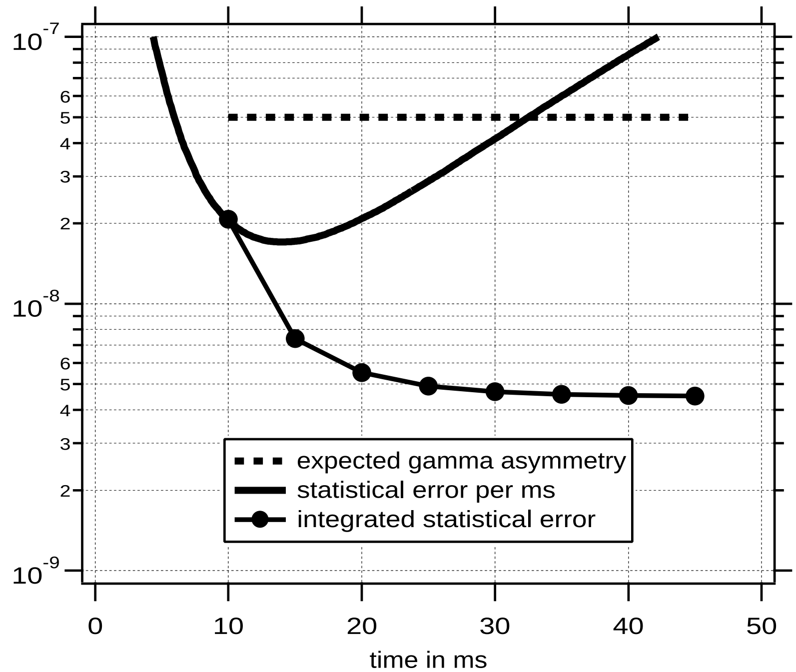

Figure 3: NPDGamma Asymmetry and Statistical Error

The NPDGamma asymmetry is small, on the order of 5×10^{-8}, and while the signal size (total counts = up plus down) is large, the difference in counts (up minus down) is small. To examine the significance of the systematic effects, we will look at the size of the difference in counts created by these effects and compare it to the size of the difference in counts for the parity-violating NPDGamma reaction. The difference in counts (u-d) for the parity-violating NPDGamma reaction is shown in figure 4. The maximum difference in counts for a single neutron pulse is only 1.5 per ms, occuring at a time of flight of approximately 13ms. Above 15meV, (below about 9ms), a neutron can suffer spin changing collisions in the liquid para-hydrogen target before capture. These collisions complicate the shape of the NPDGamma signal, and the details of the NPDGamma signal below 9ms have been omitted from the graph for the sake of clarity. The details of the depolarizing collisions above 15meV can be found in the proposal.

2 Cryostat Window

A possible source of false asymmetry for the NPDGamma experiment is the gammas emitted by beta decay from the activated cryostat window, since the asymmetry of the gammas emitted by beta decay from the activated cryostat window will be correlated with the neutron beam polarization. In order to study the size of the false signal from the cryostat window, it is necessary to calculate the temporal development of the polarization in the cryostat window. To do this it is necessary to know the time dependence of the neutron polarization and the neutron absorption in the cryostat window, the polarization transfer to the ground state of the activated cryostat window and the spin diffusion time for the polarized cryostat window. The two most likely materials for a cryostat window are aluminum and magnesium. As it turns out, pure magnesium produces a false asymmetry 4 orders of magnitude smaller than that of aluminum. However, pure magnesium is an unsuitable material for a cryostat window. A magnesium alloy has been identifed that can

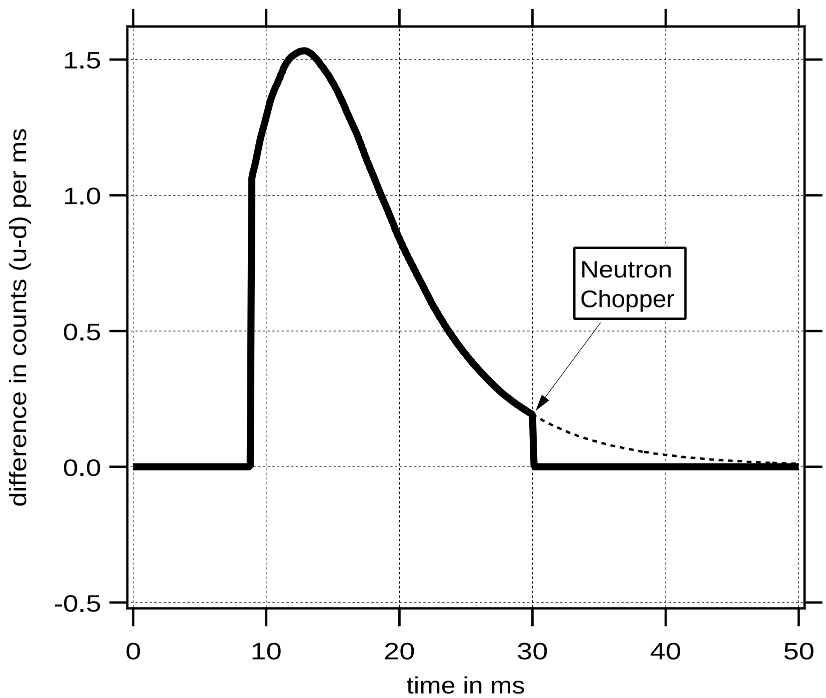

Figure 4: Experimental Difference in Counts

be used for a cryostat window; alloy AZ31B-H24 which has approxiamtely a 3% aluminum content. The false asymmetry produced by this alloy is consequently dominated by its aluminum content. If a cryostat window made from the magnesium alloy AZ31B-H24 can be made as thin as one from aluminum, then we expect the false asymmetry produced by it to be approximately 33 times smaller. Most likely, a window made from AZ31B-H24 will be slightly thicker than one made of aluminum as the tensile strength of AZ31B-H24 is 5% smaller than that of aluminum. To compare the size of the false asymmetry from the cryostat window, we will consider a cryostat window 2mm thick made from aluminum and a cryostat window 2mm thick made from magnesium alloy AZ31B-H24. For aluminum, the lifetime is 130s, and the spin diffusion time is 90ms at 20K. The ground state polarization after polarized gamma capture is 0.03. The beta asymmetry is assumed to be 1.0 and the beta to gamma conversion efficiency is 0.021. The false difference from a single neutron spill is shown in figure 5 for a 2mm aluminum cryostat window and a 2mm AZ31B-H24 cryostat window. Because of the log scale, the details of the NPDGamma signal, (which goes negative), have been omitted below 9ms. With the neutron beam chopped at 30ms, a measurement of the gammas from 30ms to 45ms will allow an in situ measurement of the gammas from activated components, which should be dominated by the gammas from the cryostat window. There are enough gammas in the 30ms to 45ms window to allow the false asymmetry from an aluminum cryostat window to be measured with an accuracy of 3%. The total difference per proton pulse for the NPDGamma reaction integrated from 9ms to 30ms is 18.867. An aluminum cryostat window would add 0.226 to that difference, while an AZ31B-H24 cryostat window would add 0.007. For an AZ31B-H24 cryostat window, a measurement of the false asymmetry in the 30ms to 45ms window could be made with a precision on the same order as the size of the effect, which is less than a 0.05% contamination to the NPDGamma signal in the 9ms to 30ms window. The numbers given so far have been for a single, isolated neutron spill. During the NPDGamma experiment, the neutron beam polarization direction will be determined using an 8-step sequence. This 8-step sequence will further reduce the size of the contamination as described in the next section.

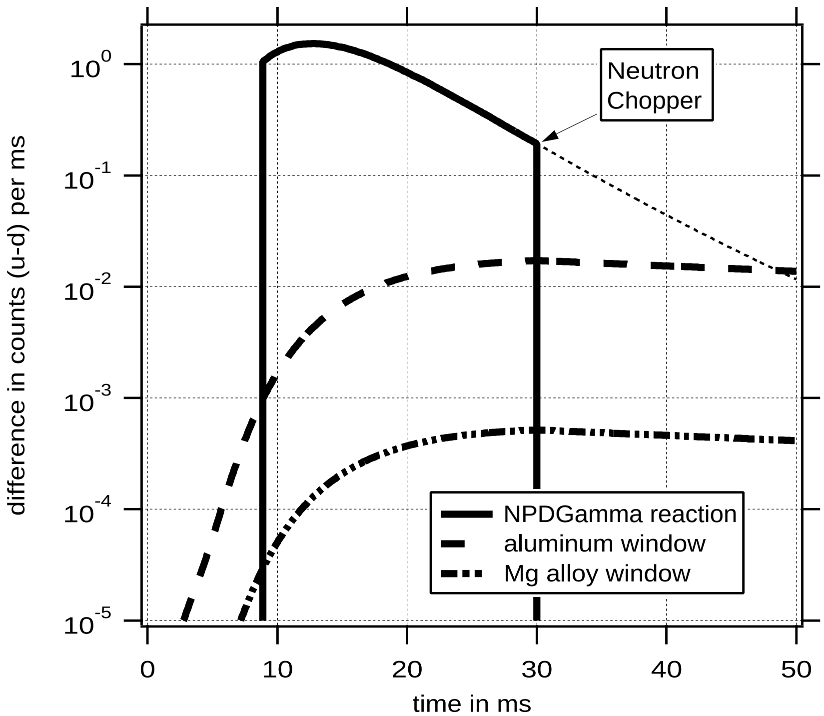

Figure 5: Experimental Difference in Counts

2.1 Neutron Spin Sequence

With a 90ms spin diffusion time in aluminum and a 50ms neutron pulse spacing, the polarization of the activated aluminum will be determined not only by the current neutron pulse, but also by the previous few neutron pulses. Figure 6 shows the polarization of the activated aluminum over an 8-step spin sequence, $(+--+-++-)$. As can be seen, the initial polarization of the activated aluminum during a neutron pulse is that of the previous neutron pulse, (which is 3 out of 4 times of the opposite sign). This is actually a benefit as it forces a zero crossing in the false asymmetry of the cryostat window at the position of the peak of the NPDGamma signal. Figure 7 shows the absolute value of the false asymmetry for the two types of cryostat windows averaged over an 8-step spin sequence. Also in the figure is the absolute value of the NPDGamma reaction. There are numerous zero crossings in the NPDGamma signal below 9ms as the neutron has enough energy at these times to undergo spin reversing collisions. In the region from 4.5ms to 9ms, the neutron has, on average, enough energy to undergo 1 spin reversing collisions. At times below that, 2 spin reversing collisions, etc... The 8-step spin sequence changes some of the details of the false asymmetry from the cryostat window and helps to reduce the size of the false asymmetry. With an 8-step sequence, the contamination from an aluminum cryostat window is reduced from 1.2% to 0.76%, and from 0.032% to 0.023% for a AZ31B-H24 cryostat window.

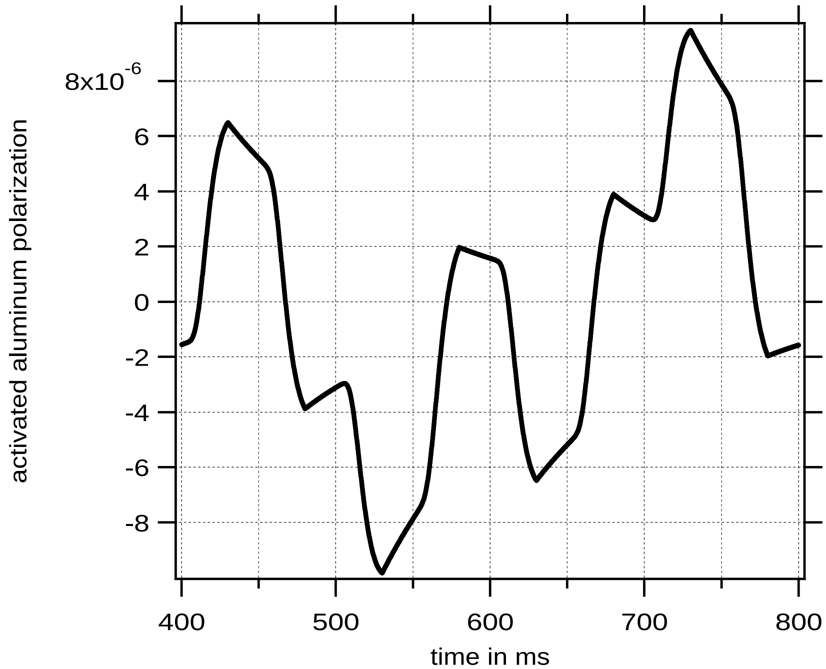

Figure 6: Activated Aluminum Polarization

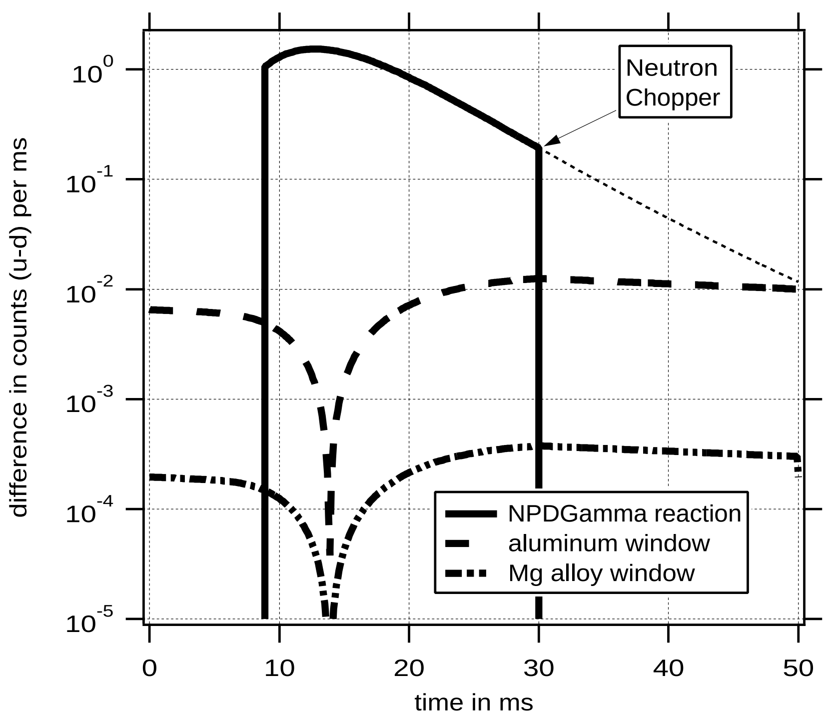

Figure 7: Experimental Difference in Counts

2.2 Conclusion

The use of the magnesium alloy AZ31B-H24 as a cryostat window for the liquid para-hydrogen target reduces the size of the false asymmetry to 2×10^{-11}, well below the expected value of 5×10^{-8} for the gamma asymmetry from the NPDGamma reaction, and well below the precision of 5×10^{-9} expected for the measurement. Through the use of a neutron chopper beginning at 30ms, the false gammas from activated components can be measured in the time of flight window from 30ms to 45ms. Using the gammas measured in this time of flight window, the value of the false asymmetry due to activated components can be calculated to a precision of 2×10^{-11}, allowing a confirmation of the size of the false asymmetry, and a verification that it is introducing a negligible contribution.

3 Systematic Effects Correlated with the Neutron Spin

As described in section 4 of the proposal, there are a number of systematic effects which are correlated with the neutron spin. The three largest of these effects are left-right asymmetries: the parity-conserving transverse analyzing power for np scattering, Mott-Schwinger scattering of the polarized neutrons in the hydrogen target, and the parity allowed left-right asymmetry in the capture reaction itself. In the limit of a perfect detector, none of these left-right asymmetries would show up in the up-down channel. However, assuming that the 48 detector elements can be aligned with an effective angle of 10 milliradians or less, then no more than 1% of the left-right asymmetries will show up in the up-down channel with the NPDGamma signal. Figure 8 shows the size of these three left-right asymmetries as well as their time dependence for an effective angle of 10 milliradians between the magnetic guide field and the detector elements. Figure 9 shows the difference in counts for the NPDGamma reaction of interest as well as the difference in counts to be expected from the three systematic effects just described at an effective detector angle of 10 milliradians. The total difference in counts for the NPDGamma reaction from 8.9 ms to 30 ms is 18.867, while elastic scattering adds 0.173, Mott-Schwinger scattering adds 0.179, and parity allowed left-right adds 0.049. If all three of these effects had the same sign, they would produce a false difference of 0.400 per neutron pulse, which is a 2.1% contamination at an effective detector angle of 10 milliradians. This should be compared to the statistical error, which is approximately 10%.

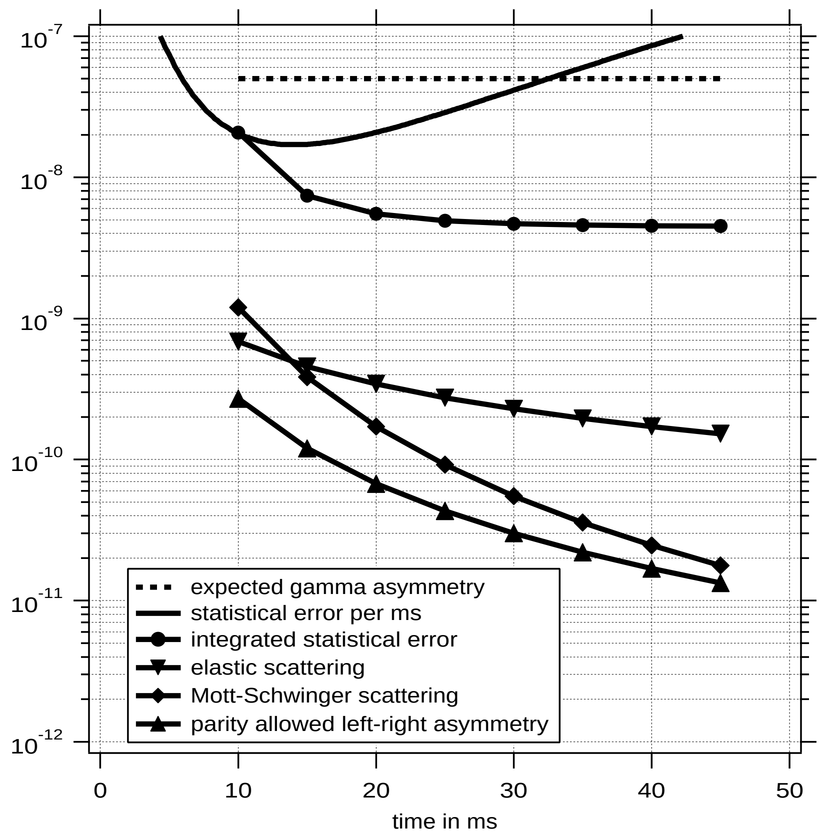

Figure 8: NPDGamma Asymmetry and Systematic Effects

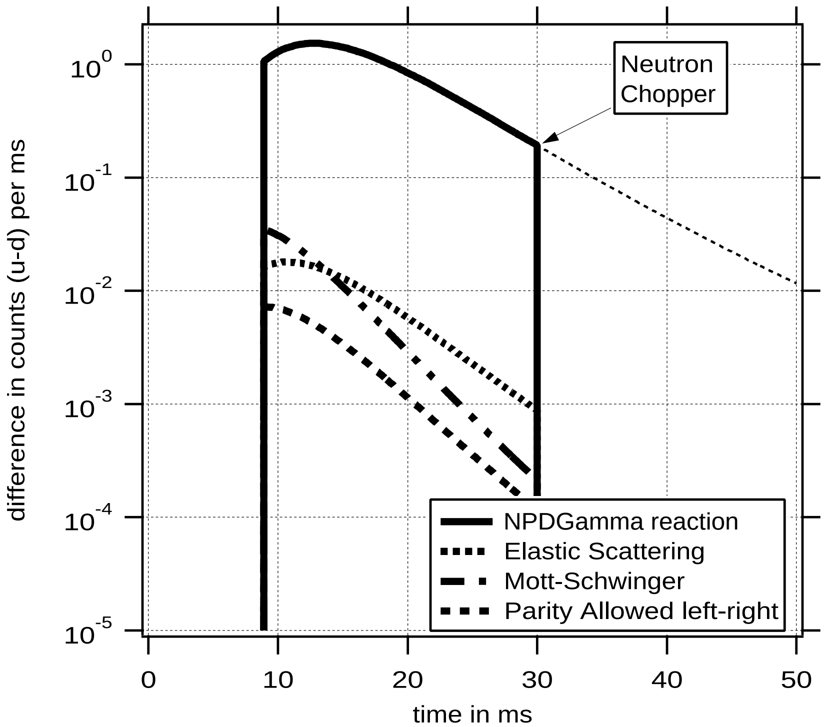

Figure 9: Difference in Counts for NPDGamma Reaction and Systematic Effects